Low-Temperature Permittivity of Insulating Perovskite Manganites

J. L. Cohn,[1] M. Peterca,[1,†], and J. J. Neumeier[2]
[1] *Department of Physics, University of Miami, Coral Gables, Florida 33124 and*
[2] *Department of Physics, Montana State University, Bozeman, Montana*

Measurements of the low-frequency ($f \leq 100$ kHz) permittivity (ε) and conductivity (σ) at $T \lesssim 150K$ are reported for $La_{1-x}Ca_xMnO_3$ ($0 \leq x \leq 1$) and $Ca_{1-y}Sr_yMnO_3$ ($0 \leq y \leq 0.75$) having antiferromagnetic, insulating ground states covering a broad range of Mn valencies from Mn^{3+} to Mn^{4+}. Static dielectric constants are determined from the low-T limiting behavior. With increasing T, relaxation peaks associated with charge-carrier hopping are observed in the real part of the permittivities and analyzed to determine dopant binding energies. The data are consistent with a simple model of hydrogenic impurity levels and imply effective masses $m^*/m_e \sim 3$ for the Mn^{4+} compounds. Particularly interesting is a large dielectric constant ($\varepsilon_0 \sim 100$) associated with the C-type antiferromagnetic state near the composition $La_{0.2}Ca_{0.8}MnO_3$.

PACS numbers: 75.47.Lx, 75.50.Ee, 77.22.Ch,77.22.Gm, 71.55.-i

I. INTRODUCTION

Recently, the lightly electron-doped manganites, e.g. $Ca_{1-x}L_xMnO_3$ (L is a Lanthanide), have been shown to exhibit a novel phase separated ground state, composed of distinct crystallographic and magnetic phases on a mesoscopic scale.[1,2,3,4,5,6] Detailed neutron diffraction studies[6] of $Ca_{1-x}La_xMnO_3$ ($x \leq 0.2$) indicate that the heterogeneity of this system is intrinsic, associated with an extremely fine balance between competing ferromagnetic (FM) double-exchange and antiferromagnetic (AF) superexchange interactions.

This paper reports investigations of the compositional dependence of the static dielectric constant (ε_0) in the Mn^{4+}-rich portion of the manganite phase diagram, accessible through low-frequency ($f \leq 100$ kHz) impedance measurements at low temperature ($T \geq 2$ K). Very few studies of the permittivity of manganites have been reported.[7,8] Specimens for which homogeneous, insulating ground states predominate are the particular focus: The A-type AF phase ($LaMnO_3$), the Wigner-crystal AF phase ($La_{1/3}Ca_{2/3}MnO_3$), the C-type AF phase ($La_{0.2}Ca_{0.8}MnO_3$), and the G-type AF phase ($Ca_{1-y}Sr_yMnO_3$). In general, ε_0 is an important parameter for models of phase separation involving the segregation of doped charge carriers on a mesoscopic scale, relevant for some compositions near to those investigated here. It is also a key parameter in determining polaronic binding energies.[9] In addition, impedance measurements provide direct information about the charge carriers since carrier hopping yields a dipolar contribution to the permittivity.

II. EXPERIMENT

Polycrystalline $La_{1-x}Ca_xMnO_3$ (LCMO) and $Ca_{1-y}Sr_yMnO_3$ (CSMO) specimens were prepared by standard solid-state reaction; the preparation methods and magnetization and transport measurements are reported elsewhere.[1,10] Powder x-ray diffraction revealed no secondary phases and iodometric titration, to measure the average Mn valence, indicates the oxygen content of all specimens falls within the range 3.00±0.01.

AC impedance measurements were conducted with an HP4263B LCR meter at frequencies $f = 100$ Hz, 120 Hz, 10 kHz, 20 kHz, 100 kHz using a 4-terminal pair arrangement. Reliable measurements of ε were restricted to $T \lesssim 160$ K where the capacitive reactance was sufficiently large ($\gtrsim 0.1\Omega$). Typical specimen dimensions were 3×1.0×0.5 mm. Silver paint electrodes were applied on the largest, polished faces of the specimens and annealed at 300 °C for 2 h to improve contact resistance. Contact capacitance can lead to apparently large values[11] of ε and thus some care is required to distinguish the true response of the sample. To rule out the influence of contacts, the impedances of several specimens were remeasured after further polishing to reduce the electrode spacing by at least a factor of two; in all cases the low-temperature data agreed within geometric uncertainties of ±10%. The results were also independent of applied DC bias from 0V-2V, and ac voltage in the range 50mV-1V.

III. RESULTS AND ANALYSIS

A. Relations

Quite generally, the complex dielectric permittivity of a solid, $\varepsilon = \varepsilon' - i\varepsilon''$, can be expressed as, $\varepsilon = \varepsilon_\infty + \varepsilon_l + \varepsilon_d$. ε_∞ is the high-frequency dielectric constant associated with displacements of ionic charge distributions relative to their nuclei. The lattice contribution, ε_l, arises from displacements of ions and their charge distributions. ε_d represents a dipolar contribution, associated in the present materials with charge-carrier hopping. ε_∞ and ε_l are generally frequency- and temperature-independent at low T. The frequency-dependent dipolar conductivity is described by a power law,[12,13] and is reflected in the

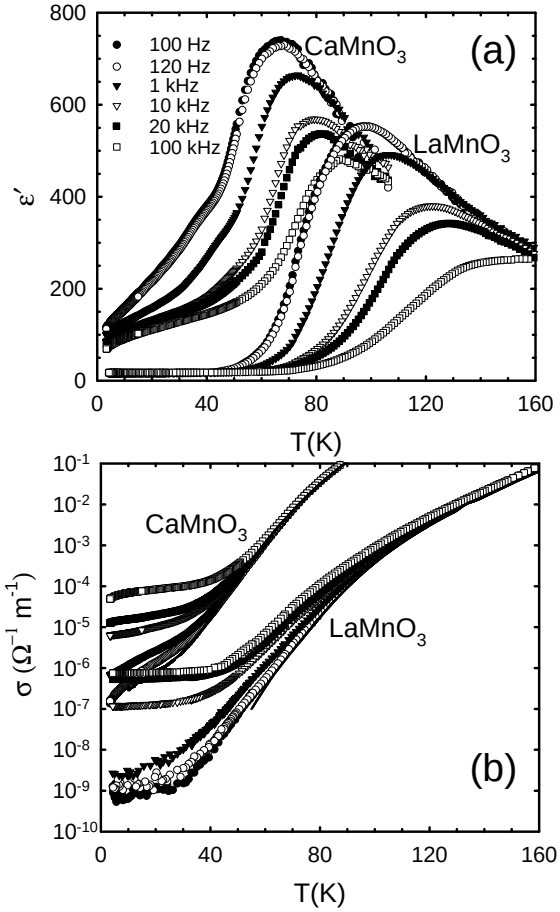

FIG. 1: (a) ε' and (b) σ *vs.* temperature for $CaMnO_3$ and $LaMnO_3$. Solid curves in (b) are dc conductivities.

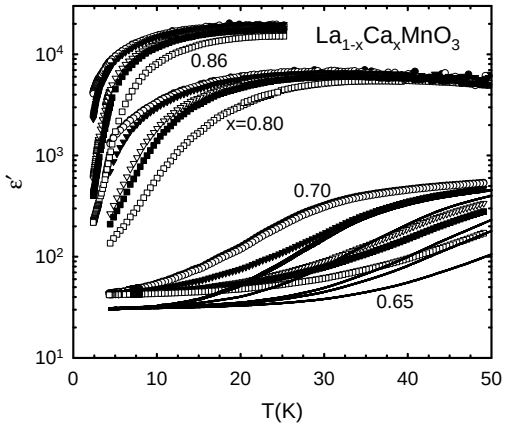

FIG. 2: $\varepsilon'(T)$ for LCMO specimens.

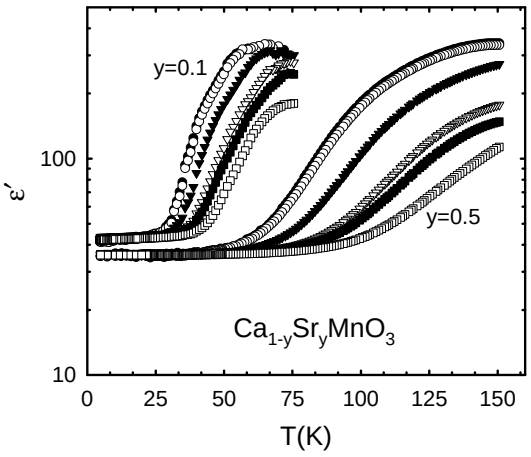

FIG. 3: $\varepsilon'(T)$ for CSMO specimens.

dielectric loss (ε_d''),

$$\sigma_d(\omega) = \sigma_0\omega^s = \omega\epsilon_0\varepsilon_d''(\omega), \tag{1}$$

where $\omega(=2\pi f)$ is the angular frequency, σ_0 is generally weakly T dependent, $s \leq 1$, and ϵ_0 is the permittivity of free space. The dipolar contribution to the real part of the permittivity (ε_d') has a characteristic frequency response that is related to that of σ_d by the Kramers-Kronig relations,

$$\omega\epsilon_0\varepsilon_d'(\omega) = \sigma_d(\omega)\tan(s\pi/2). \tag{2}$$

Dipolar relaxation effects are often evidenced in ε_d' or ε_d'' as maxima at a temperature that increases with increasing f. These features can be described empirically by the Cole-Cole expression,[14]

$$\varepsilon_d = \varepsilon_{d,\infty} + \frac{\Delta\varepsilon_d}{1+(i\omega\tau)^{1-\beta}}\ , \tag{3}$$

where $\varepsilon_{d,\infty}$ is the value of ε_d in the high-frequency limit, and $\Delta\varepsilon_d$ is the difference between low- and high-frequency limiting values. β is an empirical parameter describing (symmetric) relaxation broadening ($\beta = 0$ corresponds to monodispersive relaxation), and τ is the relaxation time.

B. Temperature Dependence of Permittivity

$\varepsilon'(T)$ and $\sigma(T)$ are shown for the end-member compounds, $LaMnO_3$ (LMO) and $CaMnO_3$ (CMO) in Fig. 1. $\varepsilon'(T)$ is shown for LCMO ($x = 0.65, 0.70, 0.80$) and CSMO ($y = 0.1, 0.50$) in Fig.'s 2 and Fig. 3, respectively.

The data for most of the specimens exhibit the canonical behavior described in the preceding section; at the lowest temperatures, ε' is independent of temperature and frequency, reflecting an intrinsic static dielectric constant, $\varepsilon_0 \equiv \varepsilon'(T \to 0)$. LMO [Fig. 1 (a)] has $\varepsilon_0 = 18$, in good agreement with values in the range 15−21 reported previously.[9,11] In this low-temperature regime, the dc conductivity is small, and the dispersive dipolar conductivity is apparent [Fig. 1 (b)]. With increasing temperature, dispersive maxima develop in ε', the signature of dipolar relaxation with a relaxation time τ that decreases with increasing T. Two sets of relaxation maxima are evident in the CMO data, the one at lower T evident as a "shoulder" in the data for the range 40−60 K. The ε' data for CMO and LCMO ($x = 0.80$, 0.84) do not reach this T-independent regime for $T \geq 2$ K, so ε_0 must be

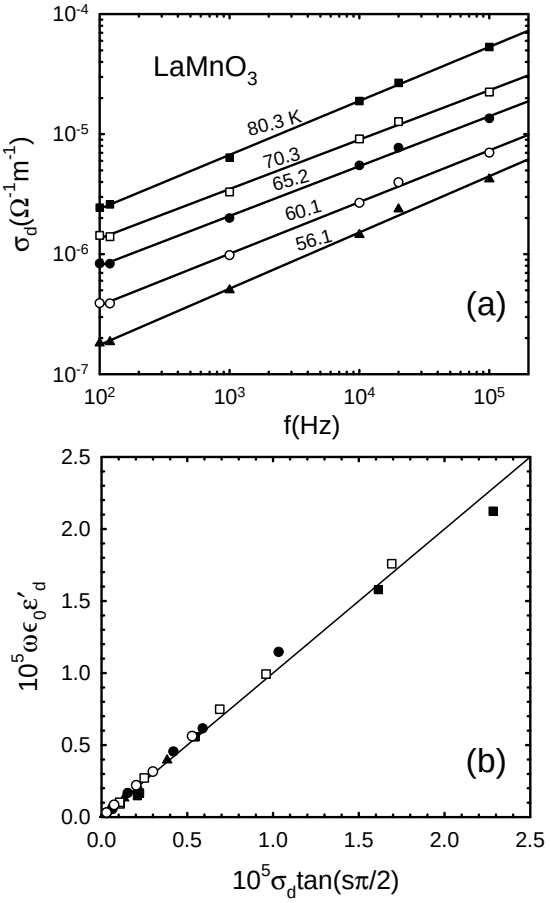

FIG. 4: (a) $\sigma_d(\omega) = \sigma(\omega) - \sigma_{dc}$ at several fixed temperatures for LMO demonstrating power-law behavior (Eq. 1). Solid lines are linear-least-squares fits. (b) $\omega\epsilon_0\varepsilon'$ *vs.* $\sigma_d \tan(s\pi/2)$ using slopes from (a). The solid line represents Eq. 2.

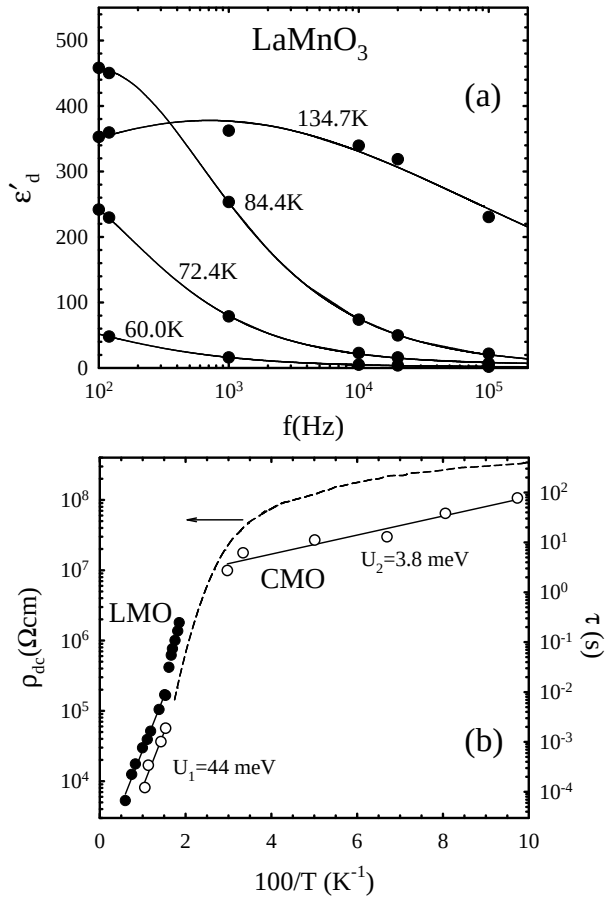

FIG. 5: (a) $\varepsilon'_d(\omega)$ at fixed temperatures for LMO. Curves are fits to Eq. 3. (b) Fitted values of τ *vs.* $100/T$ for LMO and CMO (right ordinate). Dashed curve is ρ_{dc} for CMO (left ordinate).

evaluated by extrapolation. The data for CMO are near saturation; $\varepsilon_0 = 55 \pm 6$ is estimated from the average of the $T = 0$ extrapolated values of ε' for $f = 10$ kHz, 20 kHz, 100 kHz. For $x = 0.80$ and 0.84 we employ a procedure that exploits the power-law frequency behavior for the dipolar terms as described in the next subsection.

Fig. 4 demonstrates that the dipolar contributions to ε' and σ have a common origin, consistent with charge-carrier hopping. In Fig. 4 (a), linear least-squares fits of $\sigma_d \equiv \sigma - \sigma_{dc}$ *vs.* f in a double logarithmic plot yield powers s at various T's for $LaMnO_3$. In Fig. 4 (b) these values of s and $\varepsilon'_d \equiv \varepsilon' - \varepsilon_0$ are used to verify Eq. 2.

Dipolar relaxation times, τ, were determined for all compounds by fitting $\varepsilon'(\omega)$ at fixed temperatures to Eq. 3 as shown in Fig. 5 (a) for LMO. Values of β fell in the range $0.4-0.8$, indicating a distribution of rates as is typical for hopping systems. τ is plotted against inverse temperature for both LMO and CMO in Fig. 5 (b) (for CMO, data in the regime of overlap for the two relaxation peaks were excluded). $\tau(T)$ is approximately Arrhenius-like in the accessible temperature ranges, $\tau = \tau_0 \exp(U/k_B T)$. For several compounds, two activation energies, U_1 and U_2, are defined at high- and low-T as observed for CMO. The crossover between these two relaxation regimes coincides with a crossover in the T dependence of the ac and dc resistivities [dashed curve in Fig. 5 (b)]. This behavior is characteristic of a change in the conduction mechanism from thermal activation of carriers from impurity (dopant) levels to the conduction band at high T, to impurity-band conduction at low T. This crossover is detectable in τ only for specimens having a sufficient carrier density to yield a measurable dipolar contribution to ε' extending to the low-T regime. Values of activation energies and associated values of τ_0 are listed in Table I for all compounds.

C. Compositional dependence of ε_0

To determine ε_0 for LCMO $x = 0.80$ and 0.84, we employ Eq.'s 1 and 2 which imply, $\varepsilon' = \varepsilon_0 + A\omega^{s-1}$ [$A = (\sigma_0/\varepsilon_0)\tan(s\pi/2)$ is independent of ω]. Thus plots of ε' *vs.* ω^{s-1} at fixed temperatures yield ε_0 as the common intercept (i.e., in the limit $\omega \to \infty$). At each temperature, s is determined from the frequency dependence of σ_d as in Fig. 4. This procedure is validated by appli-

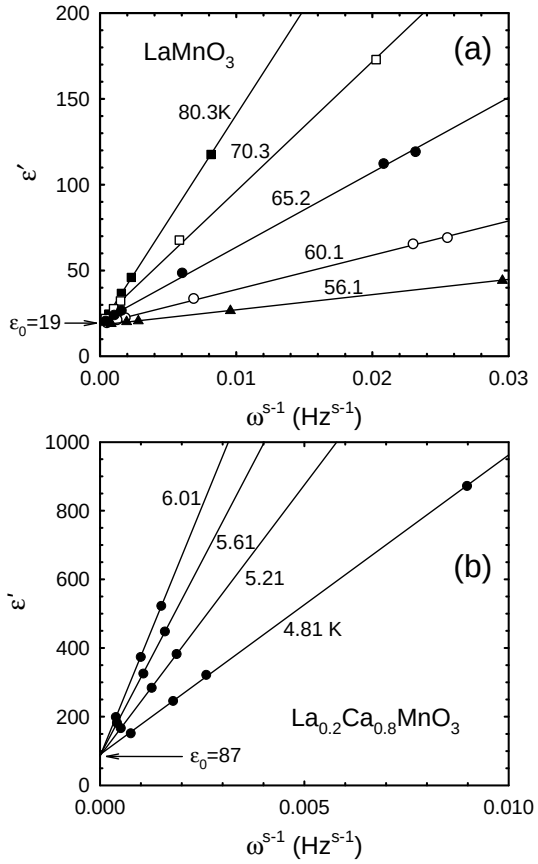

FIG. 6: ε'_d *vs.* ω^{s-1} for (a) LMO and (b) LCMO, $x = 0.8$.

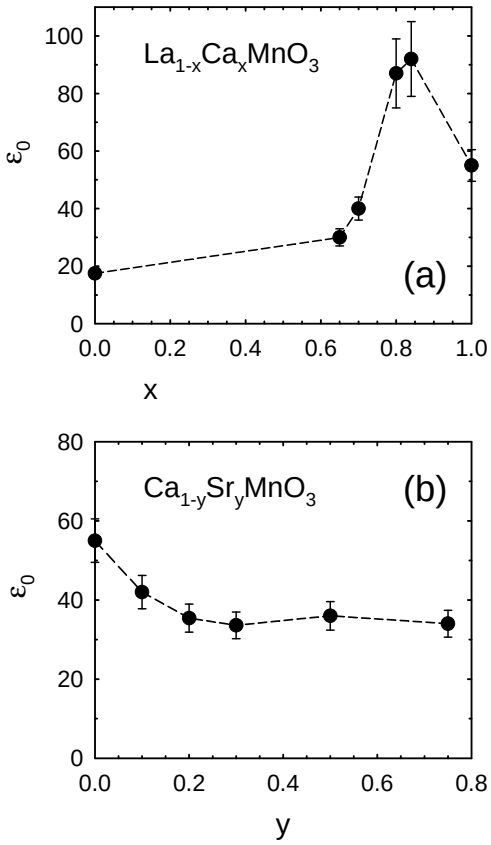

FIG. 7: Compositional dependencies of ε_0 for (a) LCMO and (b) CSMO compounds. Error bars reflect 10% geometric uncertainty with the exception of LCMO $x = 0.80, 0.84$ for which the extrapolation procedure (see text) yields a larger 14%.

cation to LMO [Fig. 6 (a)], using data at the same temperatures for which s was determined in Fig. 4 (a). The intercepts yield $\varepsilon_0 = 19 \pm 2$, in good agreement with the value $\varepsilon_0 = 18$ established from the low-T saturation of ε' in Fig. 1. Fig. 6 (b) shows results for $x = 0.80$, which yield $\varepsilon_0 = 87 \pm 12$. A similar analysis gives $\varepsilon_0 = 92 \pm 13$ for $x = 0.84$. The compositional dependencies of ε_0 for both the LCMO and CSMO compounds are shown in Fig. 7 and Table I.

IV. DISCUSSION

It is evident from the data in Table I that for the LCMO compounds (excluding CMO), larger values of ε_0 are associated with smaller values of U_1. This suggests an interpretation within a simple model for hydrogenic impurity levels for which the binding energy of donor (or acceptor) levels, which we identify as U_1, should scale inversely with the square of the dielectric constant, $U_1 = (m^*/m_e)(1/\varepsilon_0^2) \times 13.6$ eV. Figure 8 demonstrates good agreement with this simple relation for these specimens with effective mass ratios in the range $m^*/m_e \simeq 1 - 1.3$.

For the nominally Mn^{4+} CSMO compounds, ε_0 and U_1 are independent of composition within uncertainties.

TABLE I: Static dielectric constant ε_0, activation energies describing dipolar contribution from charge-carrier hopping, U_1 (high-T) and U_2 (low-T), and corresponding values of prefactors for Arrhenius relaxation times, τ_{01} and τ_{02}, from Cole-Cole fits of $\varepsilon'(\omega)$ [Eq. 3 and Fig. 5].

	ε_0	U_1 (meV)	U_2 (meV)	τ_{01} (s)	τ_{02} (s)
$LaMnO_3$	18	44	—	3.3×10^{-8}	—
$La_{0.35}Ca_{0.65}MnO_3$	31	18	4.3	1.5×10^{-5}	1.2
$La_{0.3}Ca_{0.7}MnO_3$	40	10	3.9	8.9×10^{-5}	5.6×10^{-2}
$La_{0.2}Ca_{0.8}MnO_3$	87	3.9	0.7	7.9×10^{-6}	3.3×10^{-4}
$La_{0.16}Ca_{0.84}MnO_3$	91	1.3	0.2	1.1×10^{-4}	4.6×10^{-4}
$CaMnO_3$	55	44	3.8	7.9×10^{-7}	1.0
$Ca_{0.9}Sr_{0.1}MnO_3$	42	33	—	2.2×10^{-6}	—
$Ca_{0.8}Sr_{0.2}MnO_3$	35	33	—	7.1×10^{-5}	—
$Ca_{0.7}Sr_{0.3}MnO_3$	34	31	—	3.2×10^{-3}	—
$Ca_{0.5}Sr_{0.5}MnO_3$	36	36	—	1.7×10^{-3}	—
$Ca_{0.25}Sr_{0.75}MnO_3$	34	34	—	2.8×10^{-4}	—

Using the average of these values for the five CSMO compounds in the hydrogenic impurity expression implies $m^*/m \simeq 3.2$. CMO, also nominally Mn^{4+}, appears to be an outlier. However, there is evidence that the CMO specimen has a higher carrier density than the CSMO compounds: both its higher low-T conductiv-

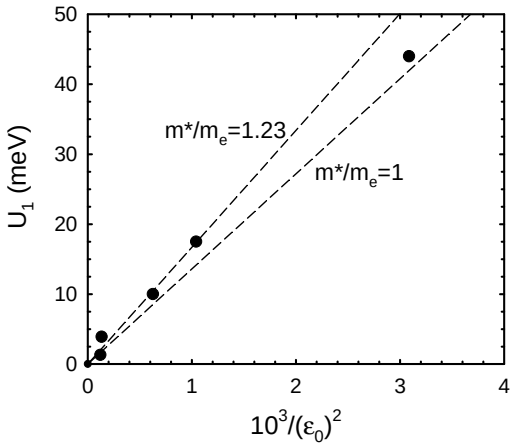

FIG. 8: Activation energy, U_1 *vs.* inverse square of ε_0 for LCMO specimens (excluding CMO). The dashed lines represent the expectation for hydrogenic impurity levels, with effective mass ratios indicated.

ity (the CSMO compounds have conductivities similar to that of LMO) and non-saturating ε' (Fig. 1). Hall coefficient measurements[17] on a similar CMO specimen yield an electron-like Hall number at room temperature, $n_H \simeq 2 \times 10^{-4}$ f.u.$^{-1} \simeq 3 \times 10^{18}$ cm^{-3}. A small oxygen vacancy concentration is a likely source of electrons, but a distribution of donors and acceptors is common in oxides. A smaller concentration of acceptors in the present compounds is expected to arise from several ppm levels of impurities (e.g., Al, Zn) in the starting chemicals. Assuming this value of n_H corresponds to full ionization of impurities, we have $N_D - N_A = n_H$ where N_D and N_A are the donor and acceptor concentrations, respectively. Donors (or acceptors) with bound electrons enhance the polarizability of a host lattice, and can plausibly account for the larger value of ε_0 observed for CMO. At low carrier density, where the donor-doped dielectric constant is not much larger than that of the undoped host (ε_h), $\varepsilon - \varepsilon_h = 4\pi N_D \alpha$, where α is the polarizability of a single donor. Taking $\varepsilon_h = 36$ (the average value for the CSMO specimens) and $N_D = n_H$ yields the reasonable value, $\alpha = 3.8 \times 10^{-19}$ cm^3.

Perhaps the most interesting results of the present work are the very large values of ε_0 observed for the two LCMO compounds, $x = 0.80$ and 0.84 [Fig. 7 (a)]. Recent neutron diffraction studies on specimens with these same compositions[6] indicate a mixture of monoclinic and orthorhombic structures at low T associated with C-type AF and Wigner-crystal (WC) type[15,16] Jahn-Teller distorted, charge- and orbitally-ordered states, respectively. Both specimens contain approximately 80% of the C-type phase. The implication is that the large values of ε_0 are associated with the monoclinic, C-type AF phase. Taking the value $\varepsilon_0 \simeq 31$ as representative of the WC phase (optimized near $x = 2/3$)[15,16], and assuming measured values of ε_0 for $x = 0.8$ and 0.84 represent weighted averages (by volume) of the values of the two component phases, a pristine C-type polycrystal is predicted to possess an even larger, $\varepsilon_0 \sim 105$. The increase of ε_0 in going from $x = 0.65$ to $x = 0.7$ suggests that the $x = 0.7$ specimen contains $\sim$ 10 % of the C-type monoclinic phase. A much smaller component of the C-type phase was also detected in structural studies on a $x = 2/3$ compound.[16]

In the absence of any known structural features (e.g., off-center atoms) that could enhance ε_0 of the C-type phase over that of the WC phase, the substantially lower values of ε_0 observed for compositions $x = 0.65$ and 0.70 suggest that the one-dimensional charge/orbital ordering that characterizes the C-type phase may play a role in determining the larger ε_0 found for $x = 0.8$ and 0.84. It is well-established from work on heavily doped Si[18] and La_2CuO_{4+y}[19] that enhancements in ε_0 by more than an order of magnitude above undoped, host-lattice values are associated with the polarizability of donors or acceptors with bound charges. The results for the latter material may be particularly relevant here because they demonstrate that, in a related class of AF oxides, this impurity-state polarizability enhancement follows the electronic anisotropy. The C-type AF state is highly anisotropic, with FM double-exchange interactions mediating a substantially higher carrier hopping rate along the direction of $d_{3z^2-r^2}$ orbital polarization, and superexchange interactions suppressing hopping in the transverse directions. It is plausible that the La-donor polarizability is correspondingly anisotropic. Thus the large ε_0 found for the $x = 0.8$ and 0.84 polycrystals could arise primarily from an enhancement of ε_0 along ($\|$) the FM chains of the C-type phase [the $(10\bar{1})$ direction of the monoclinic structure], with ε_0 in the transverse ($\perp$) directions comparable to that of the WC phase. Within this scenario, the inferred $\varepsilon_0 \sim 100$ for a C-type polycrystal would represent an average, $\sim (\varepsilon_{0_\|}\varepsilon_{0_\perp})^{1/2}$, such that $\varepsilon_{0_\|} \sim 300$. To our knowledge single crystals of the C-type compositions have not been reported, but it is clear that a study of the anisotropy of ε_0 in such materials would provide further insight into the role of the orbital order in enhancing ε_0.

V. ACKNOWLEDGMENTS

The work at the University of Miami was supported by NSF Grant No. DMR-0072276 and at Montana State University by NSF Grant No. DMR-0301166.

† present address, Physics Department, University of Pennsylvania, Philadelphia, PA

[1] J. J. Neumeier and J. L. Cohn, Phys. Rev. B **61** 14319 (2000); J. J. Neumeier and D. H. Goodwin, J. Appl. Phys. **85**, 5591 (1999).

[2] C. Martin, A. Maignan, M. Herviieu, B. Raveau, Z. Jirk, M. Savosta, A. Kurbakov, V. Trounov, G. Andr, and F. Boure, Phys. Rev. B **62**, 6442-6449 (2000); M. M. Savosta, P. Novk, M. Marysko, Z. Jirk, J. Hejtmnek, J. Englich, J. Kohout, C. Martin, and B. Raveau, *ibid.*, 9532-9537 (2000); R. Mahendiran, A. Maignan, C. Martin, M. Hervieu, and B. Raveau, *ibid.*, 11644-11648 (2000); M. Respaud, J. M. Broto, H. Rakoto, J. Vanacken, P. Wagner, C. Martin, A. Maignan, and B. Raveau, *ibid.*, **63**, 144426/1-6 (2001).

[3] P. N. Santhosh, J. Goldberger, P. M. Woodward, T. Vogt, W. P. Lee, and A. J. Epstein, Phys. Rev. B **62**, 14928 (2000).

[4] H. Aliaga, M. T. Causa, M. Tovar, A. Butera, B. Alascio, D. Vega, G. Leyva, G. Polla, and P. König, J. Phys.:cond. Mat. J. Phys.: Condens. Matter **15** 249 (2003); H. Aliaga, M. T. Causa, M. Tovar, and B. Alascio, Physica B **320**, 75 (2002); H. Aliaga , M. T. Causa, H. Salva, M. Tovar, A. Butera, B. Alascio, D. Vega, G. Polla, G. Leyva, and P. König, condmat/0010295.

[5] A. Machida, Y. Moritomo, S. Mori, N. Yamamoto, K. Ohoyama, E. Nishibori, M. Takata, M. Sakata, T. Otomo, and A. Nakamura, J. Phys. Soc. Jpn. **71**, 27 (2002); Y. Moritomo, A. Machida, E. Nishibori, M. Takata, and M. Sakata, Phys. Rev. B **64**, 214409/1-5 (2001).

[6] C. D. Ling, E. Granado, J. J. Neumeier, J. W. Lynn, and D. N. Argyriou, Phys. Rev. B **68**, 134439/1-8 (2003); E. Granado, C. D. Ling, J. J. Neumeier, J. W. Lynn, and D. N. Argyriou, *ibid.*, 134440/1-6 (2003).

[7] A. Seeger, P. Lunkenheimer, J. Hemberger, A. A. Mukhin, V. Yu. Ivanov, A. M. Balbashov, and A. Loidl, J. Phys.: Condens. Matter **11**, 3273 (1999).

[8] J. Sichelschmidt, M. Paraskevopoulos, M. Brando, R. Wehn, D. Ivannikov, F. Mayr, K. Pucher, J. Hemberger, A. Pimenov, H.-A. Krug von Nidda, P. Lunkenheimer, V. Yu. Ivanov, A. A. Mukhin, A. M. Balbashov, and A. Loidl, Eur. Phys. J. B **20**, 7 (2001).

[9] A. S. Alexandrov and A. M. Bratkovsky, J. Phys.: Condens. Matter **11**, L531 (1999).

[10] J. L. Cohn and J. J. Neumeier, Phys. Rev. B **66**, 100404/1-4 (2002).

[11] P. Lunkenheimer, V. Bobnar, A. V. Pronin, A. I. Ritus, A. A. Volvok, and A. Loidl, Phys. Rev. B **66**, 052105/1-4 (2002).

[12] M. Pollak and T. H. Geballe, Phys. Rev. **122**, 1742 (1961); S. Golin, *ibid* **132**, 178 (1963); G. E. Pike, Phys. Rev. B**6**, 1572 (1972).

[13] A. K. Jonscher, *Dielectric Relaxation in Solids,* (Chelsea Dielectrics Press, London, 1983).

[14] K. S. Cole and R. H. Cole, J. Chem. Phys. **9**, 341 (1941).

[15] M. T. Fernández-DÍaz, J. L. Martánez, J. M. Alonso, and E. Herrero, Phys. Rev. B **59**, 1277 (1999).

[16] P. G. Radaelli, D. E. Cox, L. Capogna, S.-W. Cheong, and M. Marezio, Phys. Rev. B **59**, 14440 (1999).

[17] J. L. Cohn, C. Chiorescu, J. J. Neumeier, unpublished.

[18] T. G. Castner, N. K. Lee, G. S. Cieloszyk, and G. L. Salinger, Phys. Rev. Lett. **34**, 1627 (1975); H. F. Hess, K. Deconde, T. F. Rosenbaum, and G. A. Thomas, Phys Rev. B **25**, 5578 (1982).

[19] C. Y. Chen, R. J. Birgeneau, M. A. Kastner, N. W. Preyer, and Tineko Thio, Phys. Rev. B **43**, 392 (1991).